Direct Patterning of Three-Dimensional Periodic Nanostructures by Surface-Plasmon-Assisted Nanolithography

D. B. Shao* and S. C. Chen*

Mechanical Engineering Department and Center for Nano and Molecular Science and Technology, The University of Texas at Austin, Austin, Texas 78712

ABSTRACT

The technical applications of three-dimensional (3D) nanostructures demand a fabrication technique that is convenient and yet offers design flexibility. We describe here a nanofabrication technique called surface-plasmon-assisted three-dimensional nanolithography (3D-SPAN). By utilizing optical near-field interference patterns generated by surface plasmons (SPs), we have fabricated different 2D/3D periodic polymeric nanostructures in a typical photolithography setup. We have also shown here that the nanostructures fabricated by 3D-SPAN can be controlled easily in terms of size, layout, and defects by designing the SPAN mask. Because of its design flexibility and fabrication convenience, 3D-SPAN could be used to develop "photonics on a chip", where signal processing is carried out by photons instead of electrons and be extended to other applications of direct-writing 3D functional nanostructures.

In the past decade, there has been great interest in the interactions between electromagnetic (EM) radiation and three-dimensional (3D) periodic structures with characteristic dimensions smaller than the wavelength of the radiation. The EM near field produced by such interactions alters the scattering characteristics of the subwavelength structures and thus the overall EM response. Such periodically structured materials, including photonic crystals (PhCs),[1–2] metamaterials,[3–4] and left-handed materials,[5–7] can offer unprecedented EM properties. Specifically, such periodic nanostructures responding to the optical region of the EM spectrum is of great interest; however, fabricating periodic nanostructures with such dimension scale and complexity as required with a high degree of control is very challenging. Traditional nanofabrication methods, such as electron beam (e-beam) lithography, are only capable of 2D patterning in a thin film, and the finite thickness of the film often limits their applications. A layer-by-layer stacking method[8–9] has been used to achieve 3D nanostructures; however, alignment and planarization processes between layers can be extremely complex and inconvenient. Other novel techniques have been proposed, such as a self-organizing system,[10] holographic lithography,[11] and direct laser writing (DLW) with two-photon absorption.[12] Most recently, phase-shift mask technology[13] has emerged as a promising technique for direct patterning of 3D structures. We believe that it will be vital to have a 3D nanofabrication method that possesses the following capabilities: (1) fabricating in a parallel fashion to avoid complex processes, (2) introducing local defects for desired functionalities, and (3) selectively laying out the nanostructures for microscale device development.

Surface plasmons (SPs) are collections of electrons that oscillate at an interface between a metal and a dielectric material. Because of their unusual optical properties when coupled with light, SPs have invoked immense research interest.[14] SPs cannot be generated directly by light on smooth metal surfaces because of momentum mismatch;[15] however, it has been shown that periodic nanostructures, like hole or aperture arrays, on metal films provide momentum compensation, which allows light–SP conversion and manipulation of light at subwavelength scales.[15] In fact, this phenomenon has been used to overcome the diffraction limit of traditional photolithography.[16–18] We have found that when apertures are positioned at resonant periodicities, incident light generates a strong near-field interference pattern on the opposite side of the apertures. Figure 1 shows a TM mode (with magnetic field H perpendicular to the simulation domain) distribution of optical intensity calculated by the finite difference time domain (FDTD) method. The interference pattern in the medium (refractive index $n = 1.67$) displays a pattern close to a triangular lattice with very strong intensity contrast. In our study, we chose aluminum as the

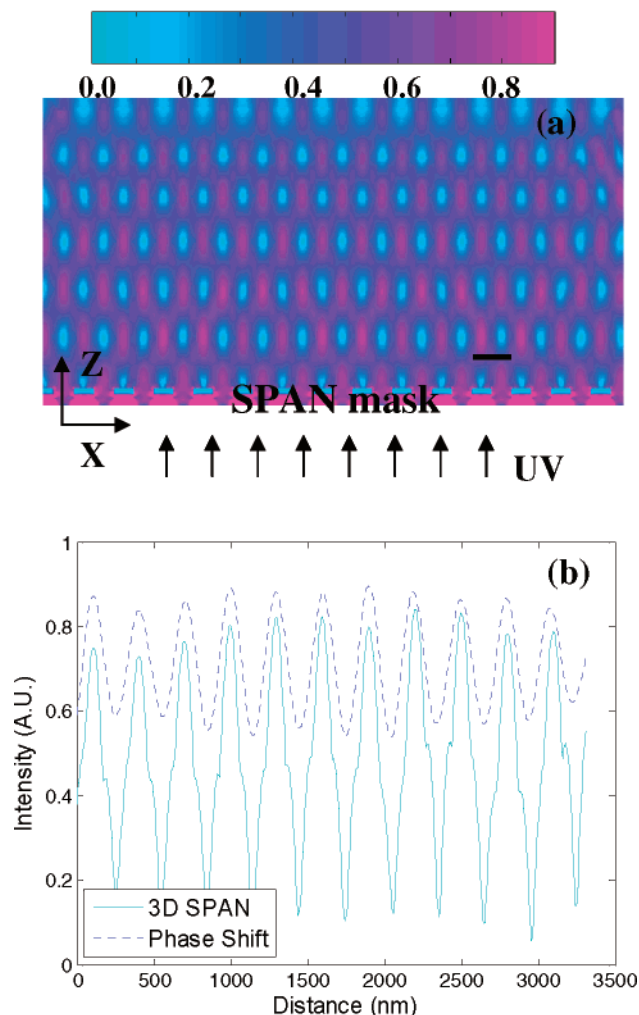* Corresponding authors. E-mail: shaochen.chen@engr.utexas.edu; Dongbing@mail.utexas.edu.

Figure 1. (a) Optical field intensity distribution in the photoresist after a 3D-SPAN mask with 1D grating. The wavelength of light is 365 nm. Scale bar = 300 nm. (b) Comparison of contrast achieved using an aluminum mask and optimized phase-shift mask.

mask material because it most strongly supports SPs at ultraviolet (UV) frequencies.[19] Our simulation results indicate that aluminum is the only common metal that can achieve such near-field interference pattern with strong contrast. The aperture width and periodicity in Figure 1 is 150 and 300 nm, respectively. It is also shown from our simulation that the periodical interference pattern is sensitive to the periodicity of the grating mask; however, the tolerance of the grating period is acceptable and within the resolution of mask fabrication by FIB lithography.

The interference pattern results from phase modulation by the mask pattern through SP−light coupling and might be related to the Wood−Rayleigh anomaly associated with the horizontal mode of SPs,[20] which is highly dependent on the grating period and the angle of incidence. Although such optical near-field interference looks similar to the ordinary diffraction grating near field, which is due to optical path difference, we believe the SPs have played an important role in our 3D-SPAN. To illustrate this point, we carried out simulation of the optical near field using a phase-shift mask with the same periodicity but varied thickness. Although the
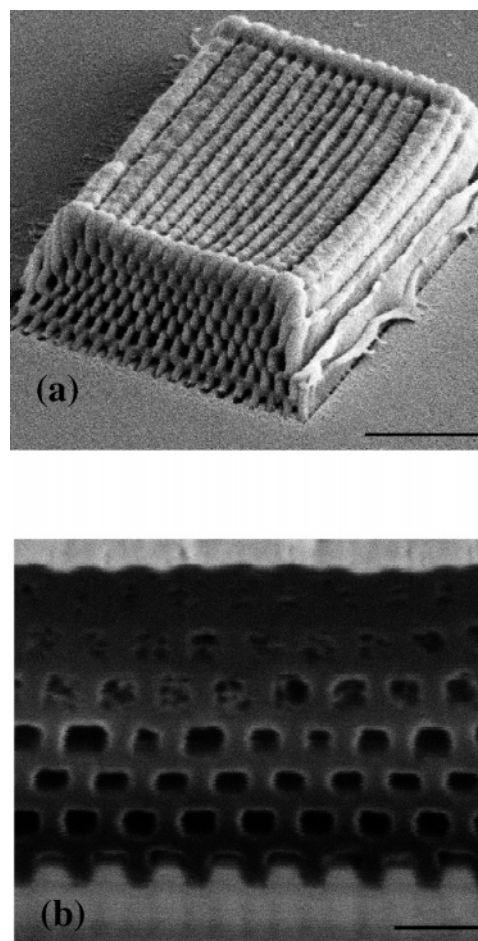

Figure 2. Structures fabricated by 3D-SPAN using 1D grating mask. (a) SEM image of the structure. Scale bar = 2 μm. (b) Cross-section view of the structure. Scale bar = 500 nm. (Note: both a and b are viewed 52° from the normal of the sample surface)

optical field patterns in the two cases are alike, the contrast is different, as shown in Figure 1b for an aluminum mask and an optimized phase-shift mask. It is clear from the plot that 3D-SPAN can achieve a much larger contrast, which can significantly facilitate the photolithography process. It is understandable that the phase-shift mask produces a relatively small contrast because the materials used in the mask are all transparent; whereas in our case the metallic material can block the undesired background light effectively. Nevertheless, we feel that the detail mechanism of SPs in achieving such high contrast interference is worth further investigation.

To transfer the optical interference pattern to the polymer structure, we used SU-8 (MicroChem), a negative tone chemically amplified photoresist. SU-8 has been used in submicrometer scale lithography for 3D structure fabrication, such as holographic lithography[11] and DLW,[12] and its unique properties qualify it for such applications. In our experiments, we first deposited a 50-nm-thick aluminum layer on a quartz substrate by e-beam evaporation. Focused ion beam (FIB) was then used to pattern the Al layer. The aluminum mask patterns include 1D grating structures, as explained previously and shown in Figure 1. After FIB patterning, SU-8 photoresist was spin-coated onto the Al mask to a thickness

of 3 μm. A thin layer of OmniCoat (MicroChem) was applied between the resist and the mask to improve adhesion. The photoresist was then exposed to UV light for 3 min through the mask using a UV aligner (HTG, 365 nm). After exposure, the samples were developed in SU-8 developer for an hour and then gently air-dried. Figure 2a shows the resulting structure viewed at a 52° angle relative to the surface normal. An SEM picture showing a cross section, cut by FIB milling, is at the same 52° angle in Figure 2b. Seven layers of holes are shown in the SEM pictures. The first layer of holes relative to the bottom of the structure does not resolve very well because of the layer of OmniCoat, while the top 3 layers are partially blocked by the material's redeposition during FIB milling. Because of the shrinkage of the SU-8 polymer, the holes are rather square instead of being elliptical, with a size of about 150 nm, and form a triangular lattice structure by self-adjustment.

The thickness of the polymer structure (the number of layers) is dependent upon several factors, among which the thickness of the photoresist and the number of grating apertures are the most important. In our experiments, a maximum of 8 layers was generated with 30 apertures and a 3-micrometer-thick photoresist. If a thicker photoresist was used, then the additional layer tended to merge because of the decrease in intensity contrast because of both diffraction and scattering in the photoresist. By optimizing the process parameters and materials used, more layers could be fabricated.

The post-exposure bake (PEB) is not implemented in the 3D-SPAN process. PEB is often used either to minimize the standing wave effect[21] or to drive the acid-catalyzed photoreaction for increased photosensitivity. For DLW,[12] the two-photon reaction rate is low so PEB must be employed. However, the elevated temperatures cause the photoproduct to diffuse and the polymer lines start merging when the distance between them is approximately half of a micrometer.[12] The 3D-SPAN technique harnesses the high-density, high-contrast interference patterns generated by SPs. As seen in our simulation, the light intensity can depreciate from 1 (incident light intensity) to 0 within about 150 nm distance. Such an intrinsically high contrast facilitates the 3D-SPAN process. Thus, PEB is not just unnecessary but rather destructive.

The side view of the 2D structure in Figure 2 matches fairly well with our FDTD simulation. However, our SPAN lithography was done using UV light from a mercury lamp, whereas in the FDTD simulation the light source is assumed to be monochromatic, polarized, and coherent. The discrepancies can be explained by the following reasons. First, the ultraviolet light from the mercury lamp has a spectrum with the maximum peak centered at 365 nm with a full width at half-maximum (fwhm) of about 20 nm. The optical properties of the materials used in 3D-SPAN, especially the aluminum mask, do not vary significantly across this UV spectrum.[22] Thus, the optical fields responding to each incoming wavelength are similar. As a result, the use of a multichromatic UV light does not significantly alter the 3D-SPAN results from what we predicted using FDTD simulation.
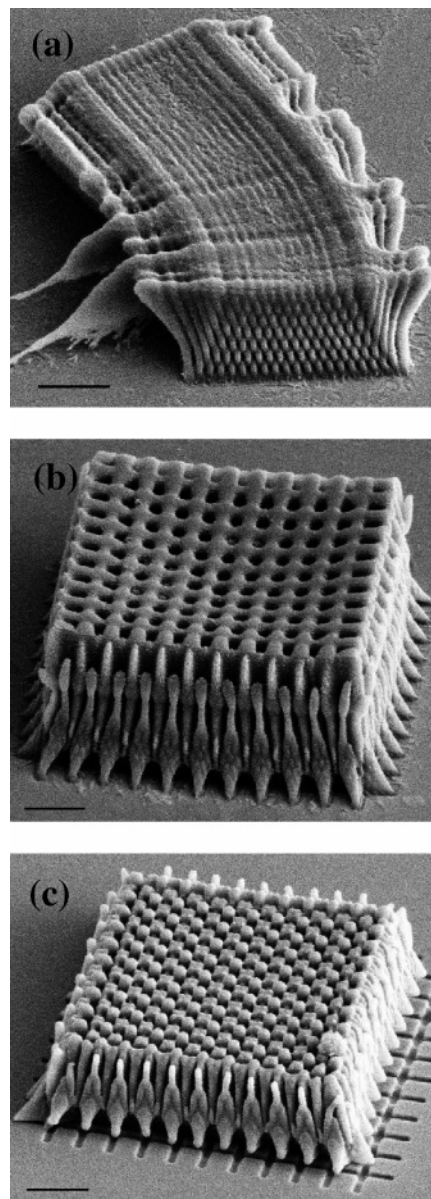

Figure 3. Different 3D structures fabricated by 3D-SPAN using a 2D grating mask. (a) A bended 2D structure. (b) A 3D structure with thickness of about 5 μm. (c) A 3D structure with thickness of about 3 μm. Scale bars = 2 μm.

Second, the unpolarized light source can be thought of as the superposition of its TM and TE components. It was found that the transmission through subwavelength metallic apertures at the TE mode is prohibited because of the absence of SP involvement;[14] thus, the contribution from the TE mode component of UV light to the lithography results is either trivial or over-shadowed by the TM mode counterpart. Finally, although the light source is incoherent, the photons are not emitted at exactly the same time. For each photon, the electrons on the aluminum mask "see" a coherent incoming EM field and cope with it accordingly. This is somewhat similar to the classical two-slit interference effect concerning white light. However, without effects from SPs transmission through the subwavelength apertures would be too low and near-field interference patterns would not be generated.
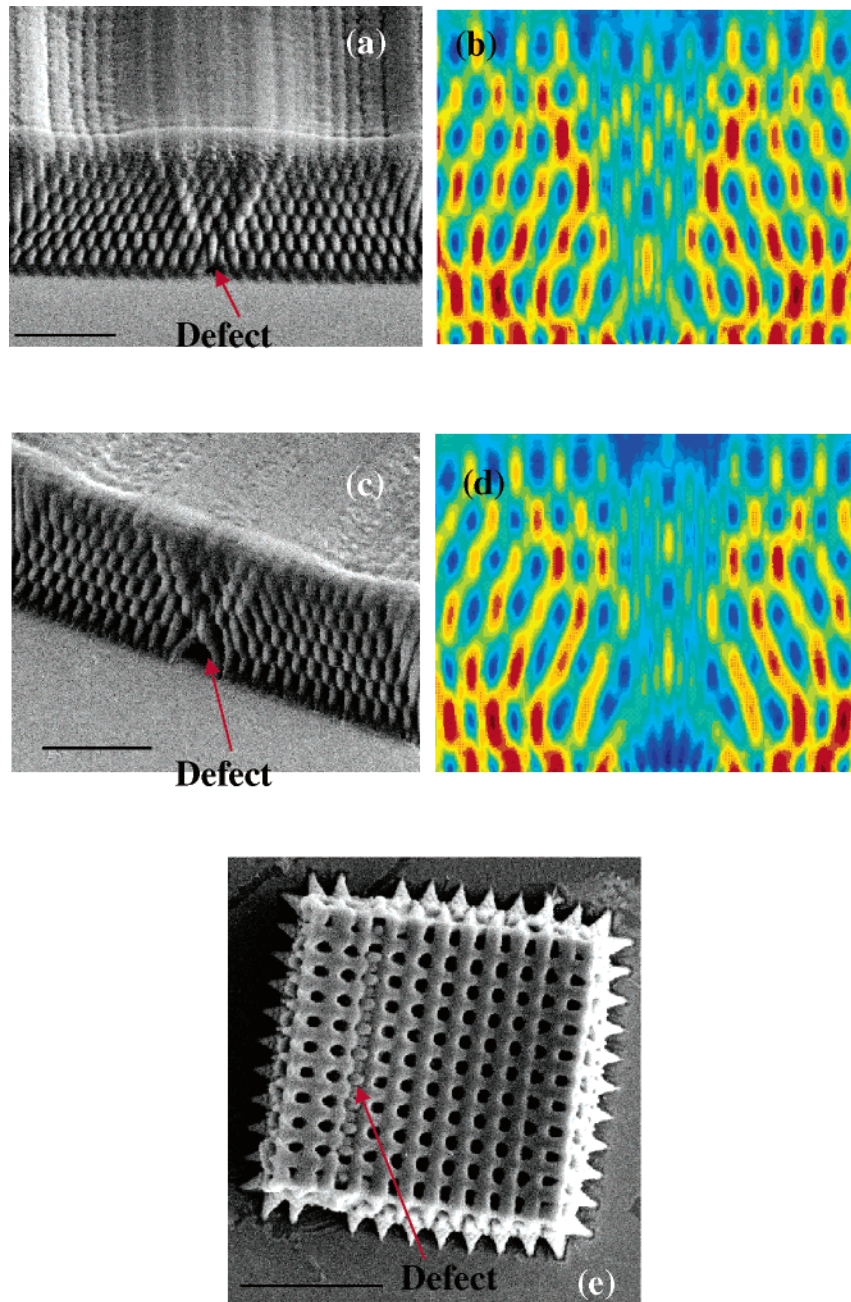
Figure 4. Different defects designed locally in the nanostructures. (a) A 2D structure fabricated using a SPAN mask with one aperture missing. Scale bar = 2 μm. (b) FDTD simulation of the corresponding condition in part a. (c) A 2D structure fabricated using a SPAN mask with two aperture missing. Scale bar = 2 μm. (d) FDTD simulation of corresponding condition in part c. (e) A 3D structure fabricated using a SPAN mask with one aperture missing. Scale bar = 5 μm.

The use of UV light rather than polarized coherent light offers advantages in terms of design flexibility. Although the pattern can only be generated with TM mode light, the unpolarized light can provide the TM component no matter how the mask pattern is oriented. What's more, the mask pattern can even be rotated and superimposed. For example, by bending the SPAN mask pattern, as shown in Figure 3a, the structure patterned in the photoresist will bend the same way. Alternatively, a cross-mask pattern, which is the superposition of two sets of 1D gratings (1 μm periodicity) that are perpendicular to each other, can be used to produce 3D structures (Figure 3b). Such 1D grating cannot produce linked structures by itself; however, the combination of them

can form elegant 3D networks. By using a thinner photoresist layer, the cross section in the z plane can be revealed, as shown in Figure 3c.

Our lithography approach resembles four-beam holographic lithography[11] in that optical interference patterns are combined with the photolithography technique to produce periodic nanostructures. However, holographic lithography creates interference by maintaining phase differences among the four beams by optical path differences, whereas in our case the interference pattern is created by an aluminum mask through which SP−light coupling occurs. Optical path difference control can be achieved only by a coherent light source with good directivity, which excludes the use of light

from a UV lamp. In addition, the 3D-SPAN process utilizes near-field interference rather than far-field interference. Although the far-field interference is more suitable for large-scale patterning of periodic structures, our approach is ideal for its nano- and microscale patterning capabilities. The dimensions of the overall structures that can be produced are as small as a few micrometers in size, which we believe cannot be achieved with equivalent quality, especially at the boundaries, by simply combining the four-beam holographic lithography with a shadow mask because of the near-field effect. Furthermore, by designing the mask layout, the 3D-SPAN technique can easily pattern nanostructures with complex outer geometries and opens the possibility of fabricating integrated nanophotonic circuits, analogous to the microelectronic circuits patterned by photolithography. Moreover, defects intentionally fabricated in periodic structures have been studied with great interest.[9] Figure 4 shows the nanostructures fabricated with 3D-SPAN masks having one or two missing apertures. We also include in the figure our FDTD modeling predictions. Considering the fact that unfastened structures will be washed away during development, we feel that the simulation is very successful in guiding our experiments. Although line and point defects may not be controlled precisely by 3D-SPAN, defects can be engineered and optimized to some extent by designing them in the SPAN mask.

The 3D-SPAN process is completely compatible with microelectronics fabrication processes. We believe that the principle of our technology can be extended to pattern photoresist film on a substrate and to pattern 3D nanostructures with overall structure dimensions much larger and more complex, provided that an appropriate mask pattern with desired dimension and quality is available. The 3D-SPAN technology then can easily allow one to replicate the 3D structures by reusing the mask. We envision our technique being used as a processing step in manufacturing components in photonics and optoelectronics. These structures can either be directly used or used as a template[10−12] to meet the fabrication needs in the nanophotonics studies.

References

(1) John, S. *Phys. Rev. Lett.* **1987**, *58*, 2486−2489.
(2) Yablonovitch, E. *Phys. Rev. Lett.* **1987**, *58*, 2059−2062.
(3) Yen, T. J.; Padilla, W. J.; Fang, N.; Vier, D. C.; Smith, D. R.; Pendry, J. B.; Basov, D. N.; Zhang, X. *Science* **2004**, *303*, 1494−1496.
(4) Smith, D. R.; Pendry, J. B.; Wiltshire, M. C. K. *Science* **2004**, *305*, 788−792.
(5) Cubukcu, E.; Aydin, K.; Ozbay, E.; Foteinopoulou, S.; Soukoulis, C. M. *Nature* **2003**, *423*, 604−605.
(6) Parimi, P. V.; Lu, W. T. T.; Vodo, P.; Sridhar, S. *Nature* **2003**, *426*, 404−404.
(7) Shalaev, V. M.; Cai, W. S.; Chettiar, U. K.; Yuan, H. K.; Sarychev, A. K.; Drachev, V. P.; Kildishev, A. V. *Opt. Lett.* **2005**, *30*, 3356−3358.
(8) Lin, S. Y.; Fleming, J. G.; Hetherington, D. L.; Smith, B. K.; Biswas, R.; Ho, K. M.; Sigalas, M. M.; Zubrzycki, W.; Kurtz, S. R.; Bur, J. *Nature* **1998**, *394*, 251−253.
(9) Qi, M. H.; Lidorikis, E.; Rakich, P. T.; Johnson, S. G.; Joannopoulos, J. D.; Ippen, E. P.; Smith, H. I. *Nature* **2004**, *429*, 538−542.
(10) Blanco, A.; Chomski, E.; Grabtchak, S.; Ibisate, M.; John, S.; Leonard, S. W.; Lopez, C.; Meseguer, F.; Miguez, H.; Mondia, J. P.; Ozin, G. A.; Toader, O.; van Driel, H. M. *Nature* **2000**, *405*, 437−440.
(11) Campbell, M.; Sharp, D. N.; Harrison, M. T.; Denning, R. G.; Turberfield, A. J. *Nature* **2000**, *404*, 53−56.
(12) Deubel, M.; Von Freymann, G.; Wegener, M.; Pereira, S.; Busch, K.; Soukoulis, C. M. *Nat. Mater.* **2004**, *3*, 444−447.
(13) Jeon, S.; Park, J. U.; Cirelli, R.; Yang, S.; Heitzman, C. E.; Braun, P. V.; Kenis, P. J. A.; Rogers, J. A. *Proc. Natl. Acad. Sci. U.S.A.* **2004**, *101*, 12428−12433.
(14) Ebbesen, T. W.; Lezec, H. J.; Ghaemi, H. F.; Thio, T.; Wolff, P. A. *Nature* **1998**, *391*, 667−669.
(15) Barnes, W. L.; Dereux, A.; Ebbesen, T. W. *Nature* **2003**, *424*, 824−830.
(16) Luo, X. G.; Ishihara, T. *Appl. Phys. Lett.* **2004**, *84*, 4780−4782.
(17) Srituravanich, W.; Fang, N.; Sun, C.; Luo, Q.; Zhang, X. *Nano. Lett.* **2004**, *4*, 1085−1088.
(18) Shao, D. B.; Chen, S. C. *Appl. Phys. Lett.* **2005**, *86*, 253107.
(19) Raether, H. *Surface Plasmons on Smooth and Rough Surfaces and on Gratings*; Springer-Verlag: New York, 1987.
(20) Collin, S.; Pardo, F.; Teissier, R.; Pelouard, J. L. *J. Opt. A: Pure. Appl. Opt.* **2002**, *4*, S154−S160.
(21) Madou, M. J. *Fundamentals of Microfabrication: The Science of Miniaturization*; CRC Press: Boca Raton, FL, 2002.
(22) Palik, E. D.; Ghosh, G. *Handbook of Optical Constants of Solids*; Academic Press: San Diego, CA, 1998.

NL061712B